Biochimie 116 (2015) 92–102

Contents lists available at ScienceDirect

Biochimie

journal homepage: www.elsevier.com/locate/biochi

Research paper

Disintegrins of *Crotalus simus tzabcan* venom: Isolation, characterization and evaluation of the cytotoxic and anti-adhesion activities of tzabcanin, a new RGD disintegrin

Anthony J. Saviola [1], Cassandra M. Modahl, Stephen P. Mackessy*

School of Biological Sciences, University of Northern Colorado, 501 20th St, CB 92, Greeley, CO 80639-0017, USA

ARTICLE INFO

Article history:
Received 2 April 2015
Accepted 4 July 2015
Available online 8 July 2015

Keywords:
Colo-205
MCF-7
Extracellular matrix
Mass spectrometry
Transcripts

ABSTRACT

Disintegrins are small non-enzymatic proteins common in the venoms of many viperid snakes. These proteins have received significant attention due to their ability to inhibit platelet aggregation and cell adhesion, making them model compounds in drug development and design investigations. The present study used a combination of molecular and proteomic techniques to screen the venom of the Middle American Rattlesnake (*Crotalus simus tzabcan*) for novel disintegrins. Six disintegrin isoforms were identified, and the most abundant, named tzabcanin, was further isolated and characterized. Tzabcanin consists of 71 amino acids, has a mass of 7105 Da (by MALDI-TOF mass spectrometry) and contains the canonical RGD binding domain. Tzabcanin was not cytotoxic to MCF-7 cells but showed weak cytotoxicity to Colo-205 cells following a 24 h incubation period. Tzabcanin inhibited cell adhesion of both cell lines to immobilized fibronectin and vitronectin, and cell adhesion to immobilized tzabcanin was inhibited when cells were incubated with a cation chelator (EDTA), indicating that integrin–tzabcanin binding is specific. This study provides a detailed analysis of the purification and characterization of tzabcanin and provides sequence and mass data for the multiple disintegrins present in the venom of *C. s. tzabcan*.

1. Introduction

Snake venoms are a complex mixture of proteins and peptides exhibiting an array of biochemical and pharmacological functions [1]. These bioactive molecules have allowed for a trophic transition from a mechanical (constriction) to a chemical (venom) means of subduing prey [2] via the dysregulation of many homeostatic mechanisms simultaneously. Because venoms consist of 'usurped' regulatory compounds, many have also been subjected to detailed screenings in the search for novel compounds which may be utilized as biomedical tools and reagents [3–5].

Disintegrins are common constituents of viperid venoms and are small (4–16 kDa) non-enzymatic, cysteine-rich proteins that result from a post-translational cleavage of the P-II class of SVMPs [6]. From a predation perspective, disintegrins may aid in the distribution of other venom compounds throughout prey tissues by binding integrins $\alpha_{IIb}\beta_3$ and inhibiting platelet aggregation [7,8]. Disintegrins may also have an important functional role during envenomation, facilitating prey relocation by altering chemical cues emanating from envenomated prey and allowing for prey recovery via strike-induced chemosensory searching [9]. Structurally, disintegrins are classified based on their polypeptide length and number of disulfide bonds [10]. Short disintegrins consist of 41–51 amino acid residues and 4 disulfide bonds, whereas medium disintegrins are approximately 70 amino acids and have 6 disulfide bonds. The vast majority of disintegrins that have been characterized and studied belong to this medium size class. The third group, long disintegrins, is composed of 84 amino acids and 7 disulfide bonds. The fourth group, which consists of the homo- and heterodimeric disintegrins, has subunits of approximately 67 amino acids, including 10 cysteines which are involved in 4 intra-chain disulfide bonds and 2 interchain cysteine linkages [10,11].

Despite the fact that disintegrins are relatively conserved, significant differences are seen with respect to their binding affinity towards integrin receptors. These disintegrin–integrin interactions are primarily mediated by the disulfide-defined integrin-binding

* Corresponding author.
E-mail address: stephen.mackessy@unco.edu (S.P. Mackessy).
[1] Current address. Department of Pharmacology, Weill Medical College of Cornell University, 1300 York Avenue, New York, NY 10065, USA.

http://dx.doi.org/10.1016/j.biochi.2015.07.005
0300-9084/

loop containing an RGD, KGD, MVD, MLD, MGD, WGD, VGD, KTS or RTS sequence [10,12–15]. Although the amino acid residues adjacent to this binding motif also influence binding affinity [16], it has been suggested that the conserved aspartate residue in the tripeptide binding site of many disintegrins is responsible for binding to the specific β integrin subunit, whereas the first two residues determine the affinity to the specific α integrin subunit [17]. The majority of characterized disintegrins contain an Arg-Gly-Asp (RGD) sequence which has been shown to block integrin $\alpha_{IIb}\beta_3$ on platelet membranes, in addition to integrins $\alpha_5\beta_1$, $\alpha_8\beta_1$, $\alpha_v\beta_1$ and $\alpha_v\beta_3$ (among others) which are expressed on many cell membranes [18]. However, non-RGD containing disintegrins have also been characterized and exhibit an array of unique integrin affinities [19,20]. These disintegrin–integrin interactions have been shown to disrupt adhesion between cells and various ECM and plasma proteins such as fibronectin, vitronectin, fibrinogen, laminin, and certain collagen [21–24].

The use of venom compounds as potential therapeutics has long been an area of interest among venom researchers. Disintegrins in particular have been explored for biomedical applications due to their potent integrin blocking activity. In fact, two anti-platelet drugs currently on the market, tirofiban (aggrastat), and integrilin (eptifibatide), were both designed based on the structures of the venom disintegrins echistatin [25] and barbourin [16], respectively. Further, disintegrins have received significant attention for their anti-metastatic and anti-angiogenic properties [21–23,26–32] demonstrating their potential applications as an anti-cancer therapeutic. RGD disintegrins such as the homodimeric contortrostatin [21,22,26], and monomeric colombistatin [23], in addition to obtustatin, which contains the sequence KTS in its active site [31,32], have been shown to significantly inhibit experimental metastasis, angiogenesis, and cellular adhesion to specific ECM proteins. The pharmacological potential of these compounds provides a strong motivation to examine snake venoms for novel disintegrins that may have application in biomedical research and drug discovery efforts.

The current study was aimed at screening the venom of the Middle American Rattlesnake (*Crotalus simus tzabcan*) for novel disintegrins by a combination of cDNA analysis of transcripts and multistep liquid chromatography and mass spectrometry-based analysis of venom proteins. We isolated and characterized the most abundant disintegrin present in *C. s. tzabcan* venom and examined its cytotoxicity and ability to inhibit cell adhesion of human colon adenocarcinoma (Colo-205) and breast adenocarcinoma (MCF-7) cell lines.

2. Materials and methods

2.1. Snakes, venom and biochemicals

Two adult *C. s. tzabcan* were housed individually at the University of Northern Colorado Animal Resource Facility (UNC-IACUC protocol #0901C-SM-ML). The snakes were received from the US Fish and Wildlife Service after a confiscation, so the exact locality of origin is uncertain; however, this subspecies occurs only in the Yucatán peninsular region of México. Venom was extracted as previously described [33], pooled, and samples were centrifuged (10,000× g for 5 min), lyophilized and stored at −20 °C until use. Matrigel (356234) was purchased from BD Biosciences (Franklin Lakes, NJ, USA). Fibronectin (F0895), vitronectin (V8379), and all additional buffers and reagents (analytical grade or better) were purchased from Sigma–Aldrich, Inc. (St. Louis, MO, USA). Protein gels, mass standards and electrophoretic reagents were obtained from Invitrogen-Life Technologies (Grand Island, NY, USA).

2.2. Size exclusion liquid chromatography (SE-LC)

Two-hundred and fifty milligrams of lyophilized venom were dissolved in 3.0 mL HEPES buffer solution (10 mM, pH 6.8, with 60 mM NaCl and 5 mM $CaCl_2$) and centrifuged at 1500× g for 5 min to pellet and remove insoluble material. This solution was then fractionated by low pressure size exclusion chromatography using a 90 × 2.6 cm column of BioGel P-100 medium (BioRad Inc., Hercules, CA, USA) equilibrated with the same HEPES buffer. Fractionation occurred at a flow rate of 6.0 mL/h at 4 °C, and 30 min fractions were collected. Elution of size-fractionated protein and peptide peaks was monitored at 280 nm using a Beckman DU640 spectrophotometer.

2.3. Reverse phase high performance liquid chromatography (RP-HPLC)

Using two additional RP-HPLC methods, peak 6 from SE chromatography was further purified using a Phenomenex Jupiter C_{18} (250 × 4.6 mm, 5 μm) column on a Waters HPLC system using Empower software. The C_{18} column was equilibrated with 95% of 0.1% TFA in water (solvent A) and 5% of 80% acetonitrile in 0.1% TFA in water (solution B) and elution was achieved as follows: 95% solvent A and 5% solvent B for 10 min; linear gradient to 85% A and 15% B over 1 min; linear gradient to 60% A and 40% B over 65 min; linear gradient to 100% B over 2 min; isocratic at 100% B for 5 min; linear gradient to 95% A and 5% B over 2 min. The peak containing tzabcanin (RP-HPLC peak 2) was further purified using the same C_{18} column and a shallower gradient. Elution was achieved as follows: 95% A and 5% B, with a linear gradient to 79% A and 21% B over 10 min; linear gradient to 75% A and 25% B over 40 min; linear gradient to 100% B over 2 min; isocratic at 100% B for 5 min; linear gradient to 100% A over 2 min; isocratic at 100% A for 5 min. Fractions were collected using a Waters Fraction Collector II at a flow rate of 1.0 mL/min, and protein peaks were monitored at 220 and 280 nm using a Waters 2487 Dual Absorbance Detector. Fractions were collected, lyophilized, and stored at −20 °C until further use.

2.4. One-dimensional SDS-PAGE electrophoresis

Crude *C. s. tzabcan* venom and SE-LC and RP-HPLC fractions were assessed for the number and relative molecular masses of protein components by SDS-PAGE under reducing (DTT) conditions using NuPAGE 12% Bis-Tris gels and MES running buffer (electrophoresed for approx. 45 min) as described previously [9]. Twenty-four μg of crude venom or 3 μL SE-LC aliquots were added to each lane, and Mark 12 standards were used for mass estimation. For RP-HPLC fractions, 3 μg of lyophilized protein were resuspended in 1× reducing LDS buffer, placed into lanes on a NuPage 12% Bis-Tris gel and electrophoresed as above. Gels were stained with Coomassie Brilliant Blue overnight, destained and scanned with an HP Scanjet 4570C.

2.5. Mass analysis (MALDI-TOF-MS) and N-terminal sequencing

Mass determinations of lyophilized protein samples obtained by RP-HPLC were analyzed using a Bruker Ultraflex MALDI-TOF/TOF mass spectrometer (Proteomics and Metabolomics Facility, Colorado State University, Fort Collins, CO) operating in linear mode. Protein samples (~0.5 μg) were spotted onto a sinapinic acid matrix (10 mg/mL 50% acetonitrile, 0.1% trifluoroacetic acid; 1.0 μL) and spectra were acquired in the mass range of 3.0–25 kDa. For N-terminal sequencing, approximately 50 μg of purified tzabcanin was reduced with dithiothreitol and alkylated with iodoacetamide

as previously described [34]. Clean up and isolation of the reduced and alkylated product was accomplished by RP-HPLC using a Vydak C_{18} column as above, with a flow rate of 1.0 mL/min and a gradient (1%/min) of 5–50% ACN. Protein fractions were collected and dried via a Speed Vac and N-terminal sequencing (Edman degradation) was performed on an ABI Procise 494 protein sequencer (Protein Structure Core Facility, University of Nebraska Medical Center, Omaha, NE) to obtain the first 30 amino acid residues. The sequence obtained was subjected to Basic Local Alignment Search Tool (BLAST) at the National Center for Biotechnology Information (http://blast.ncbi.nlm.nih.gov/Blast.cgi).

2.6. RNA isolation, cDNA synthesis and 3′ RACE

RNA isolation, cDNA synthesis, and 3′ RACE of the *C. s. tzabcan* disintegrins was accomplished following methods of Modahl et al., 2015 (in review). Briefly, RNA was purified from approximately 6 mg of lyophilized venom resuspended in 1 mL of TRIzol (Life Technologies, CA, USA) following the manufacturer's recommended RNA protocol, with the addition of a 4 °C overnight incubation in 300 μL ethanol containing 40 μL 3 M sodium acetate to increase RNA yields. cDNA synthesis from total RNA was accomplished using the 3′ RACE System (Life Technologies, CA, USA) following the manufacturer's protocols. The oligo(dT) adaptor primer (provided with the kit) initiates reverse transcriptase cDNA synthesis at the poly(A) region of mRNA and effectively selects for polyadenylated mRNAs from the total RNA preparation. Two sets of 3′ RACE sense primers were designed to obtain *C. s. tzabcan* disintegrin sequences. The first sense primer (5′-GGAGAAGARTGTGACTGTGGC-3′) was designed from the tzabcanin N-terminal sequence, and the second sense primer (5′-GAGGTGGGAGAAGAWTGYGACTG-3′) was modified from a previous primer [35] by the addition of degenerate base pairs, determined from multiple sequence alignments of a diversity of disintegrins from the NCBI database, including multiple *Crotalus adamanteus*, *Crotalus viridis viridis, Agkistrodon piscivorus, Bothrops neuwiedi, Echis pyramidum, Echis coloratus* and *Echis carinatus* metalloproteinase PII sequences. Each sense primer was used in a reaction with the 3′ RACE system AUAP antisense primer 5′-GGCCACGCGTCGACTAGTAC-3′. Twenty-three μL of PCR SuperMix High Fidelity polymerase (Life Technologies, CA, USA) was used with 1 μL of cDNA template and 0.5 μL of each primer (sense and antisense). PCR was done with seven touchdown cycles of 94 °C for 25 s, 52 °C for 30 s, and 68 °C for two minutes. Thirty additional cycles followed at 94 °C for 25 s, 48 °C for 30 s, and 68 °C for two minutes with a final 68 °C extension for five minutes. The amplified products were electrophoresed on a 1% agarose gel, and bands of the estimated disintegrin size were removed and purified using the Wizard SV gel and PCR clean-up system (Promega, USA).

2.7. Cloning and sequencing of disintegrins

Amplified cDNA was ligated into the pGEM-T Easy Vector System (Promega, Inc.) and transformed into *Escherichia coli* DH5 α competent cells and grown on nutrient-rich agar plates overnight at 37 °C. Recombinant plasmids were selected from agar plates, ten *E. coli* colonies were picked from each PCR and placed into 2 mL LB broth treated with 1 μL/mL ampicillin, and shaken overnight at 37 °C. Plasmids of each *E. coli* colony were than purified using the Quick Clean 5M Miniprep Kit (GenScript, Inc) and sent for sequencing at the DNASU facility (Arizona State University, AZ, USA) using Big Dye V3.1 chemistry with samples processed on an Applied Biosystems 3730XL Sequence Analysis Instrument.

Because snake venom disintegrins are often derived from proteolytic processing of P-II metalloproteinases, a custom BLAST database of *C. s. tzabcan* P-II SVMPs was constructed from published data [36]. The sequences obtained for disintegrins in this study were then queried against this database, and exact matches were considered P-II derived disintegrins. If sequences were 95–99%+ identical, then they were considered probably matches, and if sequences were <90% identical, they were considered not derived from P-II processing.

2.8. Cell lines and culture conditions

Cancer cells, growth media, fetal bovine serum (FBS) and cell viability assay kits were purchased from American Type Cell Culture (ATCC; Manassas, VA, USA). Human colorectal adenocarcinoma cells (Colo-205; ATCC CCL-222) were maintained with ATCC-formulated RPMI-1640 medium supplemented with 10% FBS, and human breast adenocarcinoma cells (MCF-7; ATCC HTB-22) were maintained with Eagle's Minimum Essential Medium (EMEM) growth medium supplemented with 10% FBS and 10 μg/mL human recombinant insulin. Both cell lines were maintained in 75 cm^2 flasks as a monolayer culture in a humidified 5% CO_2 air incubator at 37 °C. Subcultivation of cells was performed according to ATCC instruction, using trypsin-EDTA (0.05% trypsin and 0.02% EDTA).

2.9. Cytotoxicity assays

The colorimetric MTT [3-(4, 5-dimethylthiazolyl-2)-2, 5-diphenyl-2H-tetrazolium bromide] assay was utilized to examine possible cytotoxicity of tzabcanin, as well as crude *C s. tzabcan* venom [37]; see also 38]. One hundred μL aliquots of Colo-205 and MCF-7 cells, at a density of 5.0×10^5 cells/ml with complete media, were plated in 96-well cell culture plates and incubated with various concentrations of tzabcanin (0.22–14 μM), crude *C. s. tzabcan* venom (20 μg), or 10 μL of 0.01 M phosphate buffered saline (PBS, pH 7.2, as a control) at 37 °C for 24 h. After 24 h, 10 μL of MTT was added to the treated cells and plates were returned to 37 °C for 2 h. Following incubation, 100 μL of Detergent Reagent (ATCC) were added to cells, which were then incubated at room temperature overnight in the dark. The plate was gently shaken and the absorbance read at 570 nm using a SpectraMax 190 plate reader. Assays at each tzabcanin concentration were performed in triplicate and each assay was repeated at least twice. Percent cell viability was calculated by the following formula: [(absorbance of treatment cells) - (absorbance of medium blank)/(absorbance of control cells) - (absorbance of medium blank)] x 100, and all values are reported as mean ± standard error of the mean.

2.10. Cell adhesion inhibition assays

Inhibition of Colo-205 and MCF-7 cell binding to the extracellular matrix proteins fibronectin and vitronectin, and the basement membrane matrix Matrigel was measured as previously described [39]. Triplicate wells of Immulon-II 96 well microtiter plates were coated with either 100 μL of fibronectin (0.5 μg per well), vitronectin (0.3 μg per well), or Matrigel (0.5 μg per well) dissolved in 0.01 M PBS, pH 7.2, and allowed to incubate overnight at 4 °C. Fluid was then removed and unbound proteins were removed by washing wells three times with 1% bovine serum albumin (BSA) in PBS, and unbound sites were blocked with 2.5% BSA in PBS (1 h incubation at 37 °C). Both Colo-205 and MCF-7 cells were harvested as mentioned above and resuspended in serum-free medium containing 1% BSA at concentrations of 5×10^5 cells/mL. Cells were treated with various concentrations of tzabcanin (0.22–14 μM) and allowed to incubate at 37 °C for 1 h immediately prior to seeding. The blocking solution was aspirated, wells were washed 2× with 100 μL 1% BSA in PBS, and 100 μL cells were seeded in the coated

microtiter plate wells. Following a 1 h incubation at 37 °C, unbound cells were removed by gentle washing (3×) with 1% BSA in PBS, and then 100 μL of serum-free medium containing MTT (5:1, vol/vol) and 1% BSA was added to the wells. Following incubation at 37 °C for 2 h, 100 μL of Detergent Reagent was added to the wells and cells were incubated overnight in the dark at room temperature. The plate was gently shaken and the absorbance read as above. The percent inhibition was calculated by [(absorbance of control-absorbance of treatment)/absorbance of control] x 100. Assays at each tzabcanin concentration for all cell lines were performed in triplicate and each assay was repeated at least three times to confirm results.

2.11. Inhibition of cell binding to immobilized tzabcanin

Because integrin binding interactions are dependent on divalent cations [40,41], cells were incubated with varying concentrations of a cation chelator (disodium EDTA) to examine if tzabcanin binding occurs specifically via integrin receptors. Purified tzabcanin (20 μg/mL) was resuspended in PBS and 100 μL aliquots were add to Immulon-II 96 well microtiter plates and incubated overnight at 4 °C. Following overnight incubation, wells were washed and blocked as described above. Further, both Colo-205 and MCF-7 cells were treated as mentioned above except before addition to the disintegrin treated wells, cells were incubated for 60 min at 37 °C with serum-free medium containing 1% BSA and various concentrations of EDTA. Cells were then added to the disintegrin treated wells and the adhesion assay was performed as described above. All assays were completed in triplicate and replicated at least 3 times.

2.12. Molecular modeling

Three dimensional structure of tzabcanin was modeled from the primary structure using the I-TASSER server (http://zhanglab.ccmb.med.umich.edu/I-TASSER/) as described previously [42]. A venom disintegrin with known solution structure was identified by I-TASSER as an appropriate template model (salmosin, from *Agkistrodon halys* venom [43]: Protein Database accession number 1L3X A); tzabcanin shows 83% sequence identity with salmosin, and all 12 cysteines are conserved. Figures were created using Discovery Studio Visualizer v3.1.1.11157 (Accelerys Software Inc., San Diego, CA).

2.13. Statistical analyses

Data were analyzed by Analysis of Variance (ANOVA) followed by Tukey's post-hoc test using R version 2.15.2. All p values <0.05 were considered as statistically significant.

3. Results

3.1. Isolation and masses of C. s. tzabcan disintegrins and N-terminal sequencing of tzabcanin

Following SE chromatography, 9 major peaks were collected (Fig. 1) which were assessed by reduced SDS-PAGE (Fig. 1 inset) to identify proteins in the ~7 kDa range, as this is the general mass of monomeric disintegrins [11,23,24,27]. Peak 6 yielded one protein band in this mass range (Fig. 1 inset), and was further fractionated by RP-HPLC chromatography, yielding 5 additional protein fractions that eluted between 22 and 28% solution B (Fig. 2A). Following reducing SDS-PAGE, all five fractions showed masses of approximately 7 kDa (Fig. 2A). The spectra obtained by MALDI-TOF indicated the presence of six disintegrin isoforms in *C. s. tzabcan* venom (Fig. 2B). The most prominent of these disintegrins (RP-HPLC Peak

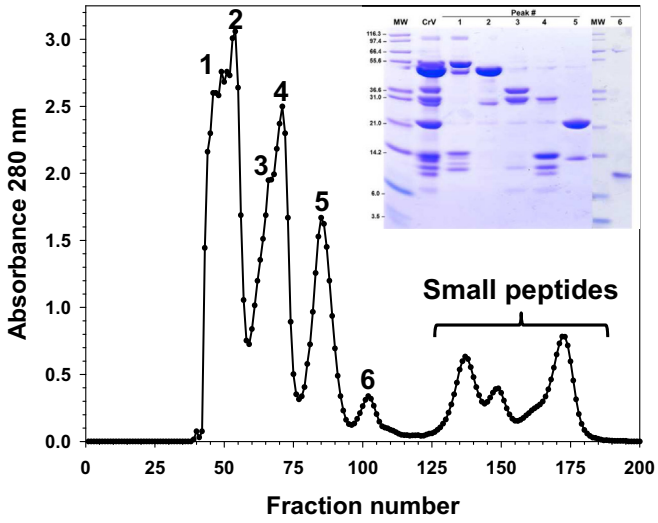

Fig. 1. Size exclusion chromatography of crude *C. s. tzabcan* venom. A total of 250 mg of crude venom was fractionated on a BioGel P-100 column. Fractions collected and crude venom (CrV) were analyzed by SDS-PAGE (inset) under reducing conditions; fraction 6 contained disintegrin-sized peptides.

2) was further purified by an additional RP-HPLC step (Fig. 3A), yielding one protein peak eluting at approximately 23% solvent B. This protein, with a molecular mass of 7105.0 Da (Fig. 3B), was named tzabcanin. It was subjected to Edman degradation N-terminal sequencing, yielding the sequence GEECDCG-SPANPCCDAATCKLRPGAQCADGLCCD and was assessed for cytotoxicity and inhibition of Colo-205 and MCF-7 cell adhesion to fibronectin, vitronectin and Matrigel.

Because MALDI-MS determinations of masses of disintegrin peaks did not correspond to theoretical masses derived from cDNA sequences (likely due to C-terminal truncation; see Discussion), cDNA-derived sequences were analyzed using ExPasy's ProtParam tool (http://web.expasy.org/protparam/) to predict sequence association with the RP-HPLC chromatogram. Based primarily on hydropathicity values (less negative values correlate with increased hydrophobicity), sequences were tentatively assigned to the respective HPLC peaks (Table 1).

3.2. cDNA sequencing analysis

Six cDNA sequences were obtained, ranging from 210 to 222 bp in length and coding for six protein isoforms varying from 69 to 73 amino acids (Fig. 4).

NCBI Protein BLAST analyses indicated that all amino acid sequences obtained belong to the disintegrin family. Five of the six sequences contain twelve cysteine residues, characteristic of medium sized disintegrins [28]; tzbdis-4 contains only 11 cysteine residues. All six sequences also express the canonical RGD binding motif.

The six disintegrins and the N-terminal sequence of tzabcanin were aligned with sequences of disintegrins purified from other viperid venoms (Fig. 5). Tzabcanin, the most abundant of the six disintegrin isoforms, contains 71 amino acids, begins with a Gly, ends with an Ala, and shares 97% sequence identity to the disintegrin basilicin [P31981].

3.3. Cytotoxicity

Crude *C. s. tzabcan* venom (20 μg/100 μL) exhibited potent cytotoxicity towards both Colo-205 and MCF-7 cell lines, with approximately 35 and 26% cell viability, respectively, remaining

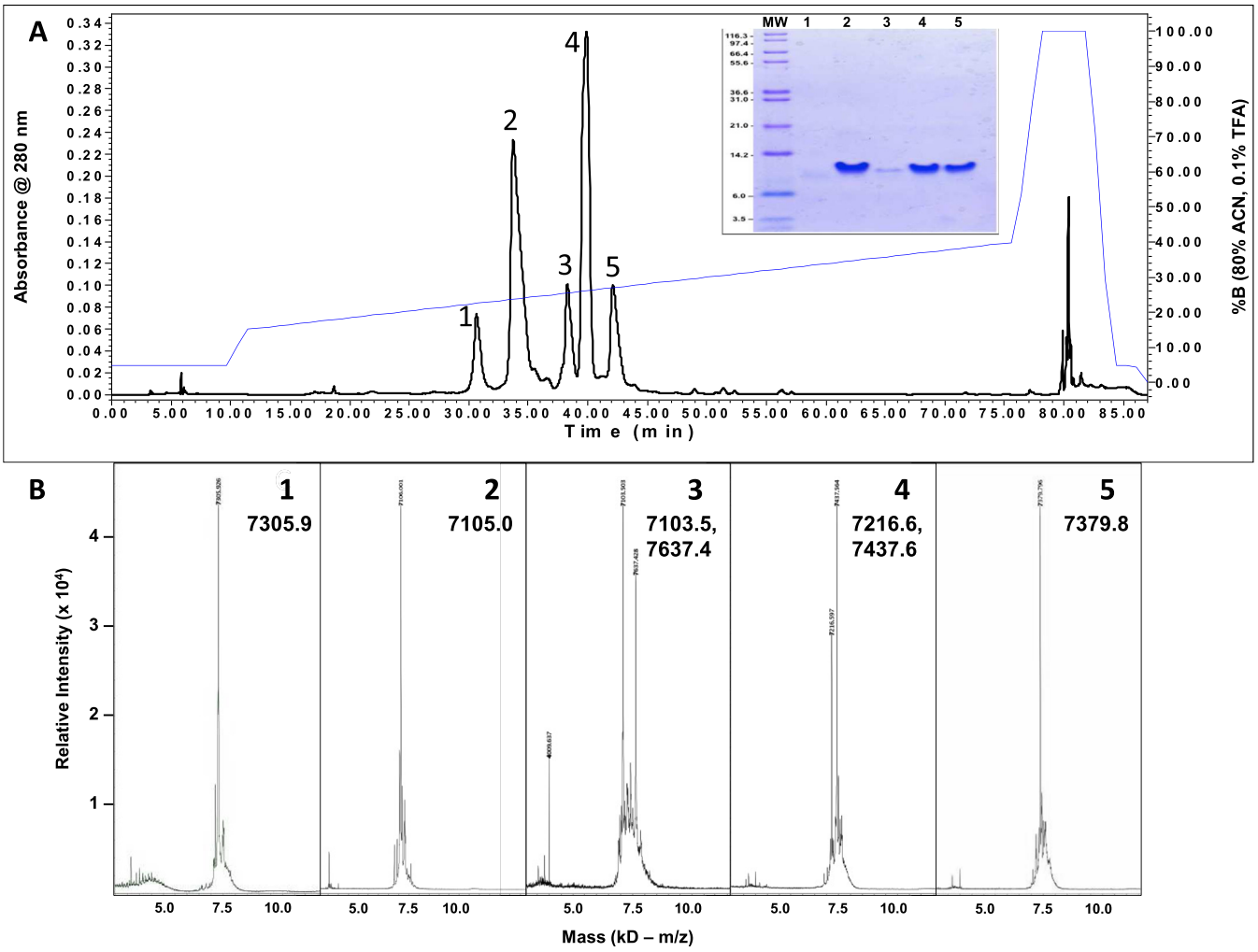

Fig. 2. RP-HPLC purification and mass determination by MALDI-TOF-MS of *C. s. tzabcan* venom disintegrins. (A) RP-HPLC of SE peak 6. 2 mL samples were injected into a Phenomenex Jupiter C_{18} column and separated on a Waters 515 HPLC system. Five protein peaks eluted between 22 and 26% solvent B. Fractions were collected and analyzed by SDS-PAGE (inset) under DTT-reducing conditions. (B) Mass spectra of RP-HPLC peaks 1–5; tzabcanin was present in peak 2 (m = 7105 Da), and peaks 3 and 4 yielded two masses as indicated.

after 24 h incubation (both $p < 0.001$; Fig. 6). However, tzabcanin caused only a slight decrease in Colo-205 cell viability at concentrations of 1.75 μM and 3.5 μM (both $p < 0.05$) and at 14 μM ($p < 0.01$); 7 μM tzabcanin also resulted in a decrease in cell survival, but this treatment level failed to reach significance ($p > 0.05$).

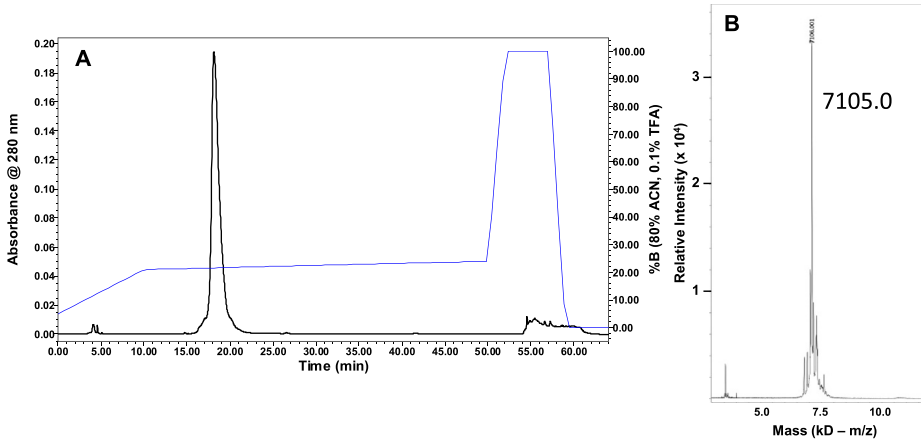

Fig. 3. RP-HPLC polishing and mass determination of tzabcanin. (A) RP-HPLC peak 2 was further purified using a very shallow gradient. One peak eluted at 23% ACN and was assessed by MALDI-TOF mass spectrometry. (B) Mass determination of tzabcanin by MALDI-TOF mass spectrometry analysis in positive linear mode indicated a native mass of 7105 Da.

Table 1
Grand average of hydropathicity (GRAVY) and other physical parameters for *C. s. tzabcan* disintegrins.

RP-HPLC peak#	Hydropathicity value	pI	cDNA sequence#	# aas	PII-derived?
1	−0.799	7.61	1	71	No
2 (tzabcanin)	−0.754	6.84	2	71	No
3	−0.674	4.81	4	73	Yes?
4	−0.592	4.81	6	73	Yes?
5	−0.578	4.58	5	73	Yes
–	−0.565	5.03	3	69	Yes

Values calculated with ExPasy ProtParam tool. #aas, number of residues in disintegrin; PII-derived?, disintegrin derived from P-II SVMP: yes? = probable. See text for further explanation.

Tzabcanin failed to exhibit significant cytotoxicity towards MCF-7 cells ($p > 0.05$).

3.4. Inhibition of cell adhesion in vitro

Fibronectin and vitronectin support adhesion to Colo-205 and MCF-7 cells. Results indicate that tzabcanin inhibits adhesion of both cell lines to fibronectin and vitronectin in a dose-dependent manner (Fig. 7a and b). The greatest inhibition was observed for MCF-7 cells binding to fibronectin (81% binding inhibition at 14 μM; IC_{50} = 6.9 μM), and although adhesion of Colo-205 cells to fibronectin was hindered, the IC_{50} was twice as high (14 μM).

Similarly, tzabcanin inhibited adhesion of both cell lines to vitronectin (Fig. 7B); the highest binding inhibition was observed with Colo-205 cells (62% binding inhibition at 3.5 μM; IC_{50} = 6.6 μM), but inhibition of MCF-7 cell adhesion failed to reach 50% (44% binding inhibition at 14 μM). Matrigel supported adhesion in both cell lines, but tzabcanin failed to inhibit adhesion (data not shown).

3.5. Tzabcanin binds to Colo-205 and MCF-7 cells via integrin(s)

Binding of both Colo-205 cells and MCF-7 cells to immobilized tzabcanin was inhibited when cells were incubated with varying concentrations of EDTA (Fig. 8). Approximately 95% inhibition of MCF-7 cell binding to immobilized tzabcanin was achieved at 5 mM EDTA (IC_{50} = 2.01 mM), and 55% binding inhibition of Colo-205 cells to tzabcanin was achieved at 5 mM EDTA. These results suggest that tzabcanin binds to both of these cell lines via integrin receptors.

3.6. Molecular modeling of tzabcanin

Like other medium disintegrins, tzabcanin adopts a semi-globular configuration, and the RGD integrin-binding domain is presented on the surface of the molecule (Fig. 9). The accessibility of this integrin-binding loop is believed to be critical to the binding efficiencies of disintegrins; a similar integrin-binding motif is found in the disintegrin-like domain of many P-III SVMPs [44] and is also likely functionally very important [45]. In addition, the model indicates close proximity of both the N- and C-termini to the RGD site; as the C-terminus has been implicated in the selectivity of disintegrins [13], this conformation likely has functional significance as well.

4. Discussion

Due to their potential as lead compounds for binding and blocking integrin receptors, disintegrins have become one of the most studied venom protein families to date. In the current study, a combination of molecular and proteomic techniques were utilized to screen the venom of *C. s. tzabcan* for potentially novel disintegrins. SE peak 6 yielded one protein mass of approximately 7–8 kDa by SDS-PAGE and was subjected to an additional RP-HPLC step, yielding 5 additional protein peaks, each exhibiting molecular masses in the range of monomeric disintegrins as determined by both SDS-PAGE and MALDI-TOF mass spectrometry. When combined with cDNA analyses, results indicate the presence of numerous disintegrin isoforms with masses ranging from 7105 to 7637 Da, and 69 to 73 amino acids in length. The molecular masses, cysteine pattern, and polypeptide length place these disintegrins in the medium-size classification as described by Calvete et al. [10,11]. Sequences obtained via cDNA analyses were tentatively assigned to the 5 peaks resulting from RP-HPLC fractionation of BioGel peak 6 based on their elution profile and GRAVY values (see Table 1). However, although MALDI-TOF mass analysis also indicates the presence of six isoforms which correlate with these six cDNA sequences, caution must be taken when interpreting this assignment of the RP-HPLC peaks to the specific translated amino acid sequences reported here without further independent amino acid sequence data (MS/MS or Edman degradation). Only RP-HPLC peak two, the most abundant of the disintegrins present, was further characterized by N-terminal sequencing and definitively assigned to the complete amino acid sequence obtained from cDNA sequences.

As has been observed for other snake venom disintegrins, including from the related *Crotalus simus* [24], theoretical and MALDI-MS-derived masses did not agree. It is hypothesized that this difference may result from the C-terminal truncation of tzabcanin; the mass of tzabcanin lacking the last four residues is 7098.94, which differs from tzabcanin's MALDI-determined mass by 0.08%. This difference is well within the margin of error (~0.1% - for example, University of Virginia School of Medicine MS core facility) often claimed for MALDI-TOF-MS. C-terminal loss of residues was also noted in a previous study of dimeric disintegrins, in which both subunits lost residues [46], so C-terminal truncation may not be particularly uncommon among some snake venom disintegrins. It may also explain the somewhat lower potency of tzabcanin toward cell adhesion inhibition than has been observed for other related disintegrins.

Tzabcanin, the most abundant of the six isoforms, shares high amino acid sequence identity with basilicin from *Crotalus basiliscus* venom. Basilicin has an additional alanine at the N-terminus, a Glu at position 29 and Lys at position 43, whereas tzabcanin contains an Asp and Thr at these positions, respectively. Both disintegrins also have identical RGDN and C-terminal sequences. Molecular modeling of tzabcanin demonstrates that the RGD binding motif, as well as the C-terminus, are accessible to the solvent and are therefore available for integrin binding. Binding specificity and affinity is based on the functional epitope created by the concerted actions of the tripeptide binding loop and the C-terminal region of the protein [13]. Further, the amino acid residues flanking the tripeptide sequence can greatly influence integrin affinity [11,13,47]. For example, disintegrins expressing RGDW domains often show

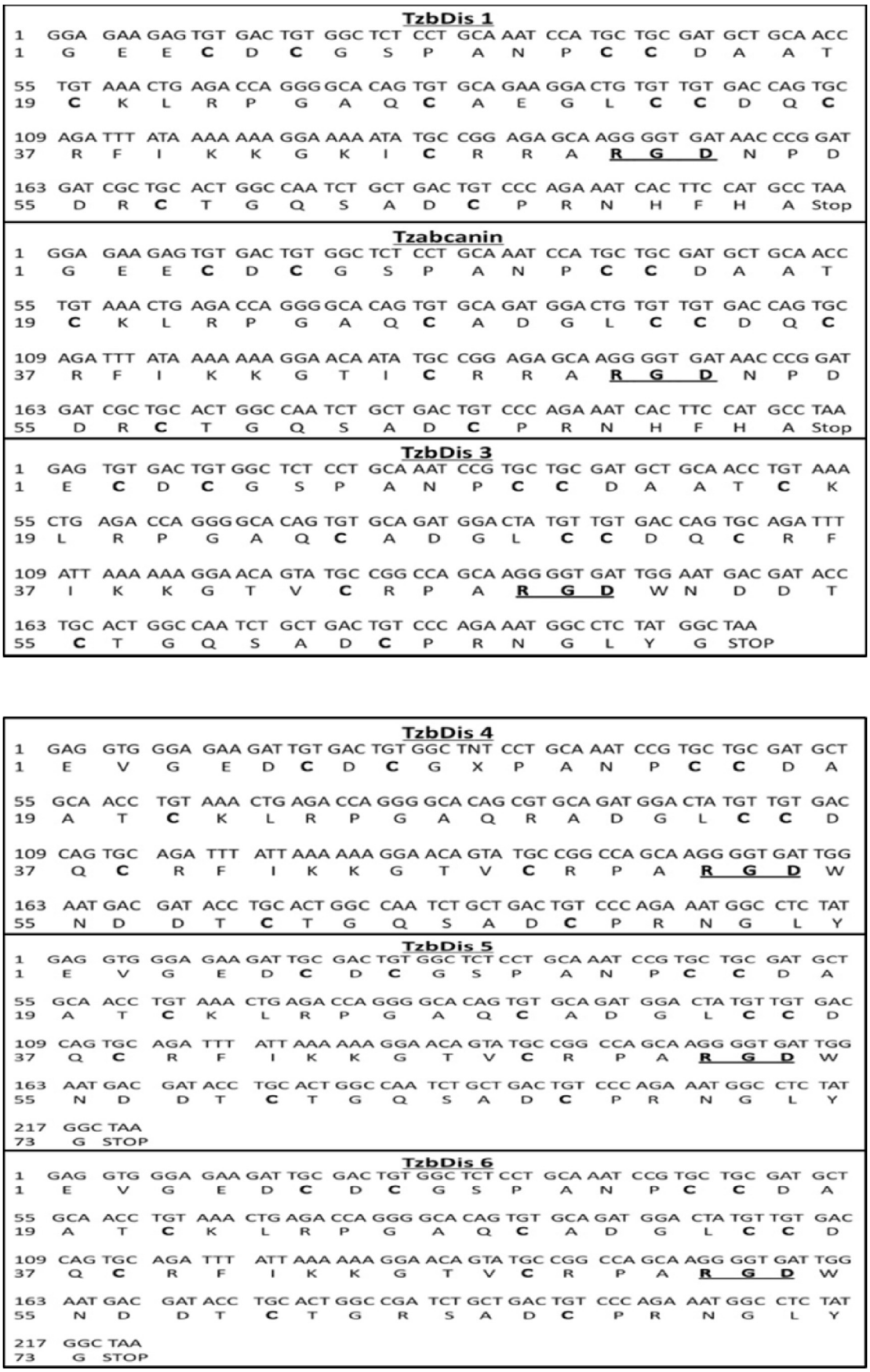

Fig. 4. cDNA sequence and predicted amino acid sequence of *C. s. tzabcan* disintegrins. The cDNA sequence is located on the upper line and the corresponding amino acid sequence is below. The cysteine residues are in bold print and the RGD binding motif is in bold print and underlined.

```
N-Terminal                  --GEECDCGSPANPCCDAATCKLRPGAQCADGLCCD----------------------------------
Tzabcanin                   --GEECDCGSPANPCCDAATCKLRPGAQCADGLCCDQCRFIKKGTICRRARGDNPDDRCTGQSADCPRNHFHA
Tzbdis-1                    --GEECDCGSPANPCCDAATCKLRPGAQCAEGLCCDQCRFIKKGKICRRARGDNPDDRCTGQSADCPRNHFHA
Basilicin [P31981]          -AGEECDCGSPANPCCDAATCKLRPGAQCAEGLCCDQCRFIKKGKICRRARGDNPDDRCTGQSADCPRNHFHA
Molossin [P31984]           EAGIECDCGSPENPCCDAATCKLRPGAQCADGLCCDQCRFIKKGKICRRARGDNPDDRCTGQSADCPRNRFHA
Viridin [P31987]            -AGEECDCGSPANPCCDAATCKLRPGAQCAEGLCCDQCRFIKKGKICRRARGDNPDDRCTGQSADCPRNRFH-
Cereberin [P31985]          EAGEECDCGSPANPCCDAATCKLRPGAQCAEGLCCDQCRFIKKGKICRRARGDNPDDRCTGQSADCPRNRFH-
Virdistatin-2 [AEY81222]    EAGEECDCGSPANPCCDAATCKLRPGAQCAEGLCCDQCRFIKKGKICRRARGDNPDDRCTGQSADCPRNRFHA

Tzbdis-3                    ----ECDCGSPANPCCDAATCKLRPGAQCADGLCCDQCRFIKKGTVCRPARGDWNDDTCTGQSADCPRNGLYG
Simusmin [C0HJM4]            AGEECDCGSPANPCCDAATCKLRPGAQCADGLCCDQCRFIKKGTVCRPARGDWNDDTCTGQSADCPRNPFH
Cerastin [P31982]           EAGEECDCGTPENPCCDAATCKLRPGAQCADGLCCDQCRFMKKGTVCRVARGDWNDDTCTGQSADCPRNGLYG
Barbourin [P22827]          EAGEECDCGSPENPCCDAATCKLRPGAQCADGLCCDQCRFMKKGTVCRVAKGDWNDDTCTGQSADCPRNGLYG
Tzbdis-4                    EVGEDCDCGSPANPCCDAATCKLRPGAR-ADGLCCDQCRFIKKGTVCRPARGDWNDDTCTGQSADCPRNGLYG
Tzbdis-5                    EVGEDCDCGSPANPCCDAATCKLRPGAQCADGLCCDQCRFIKKGTVCRPARGDWNDDTCTGQSADCPRNGLYG
Tzbdis-6                    EVGEDCDCGSPANPCCDAATCKLRPGAQCADGLCCDQCRFIKKGTVCRPARGDWNDDTCTGRSADCPRNGLYG
Crotatroxin [P68520]        -AGEECDCGSPANPCCDAATCKLRPGAQCADGLCCDQCRFIKKGTVCRPARGDWNDDTCTGQSADCPRNGLYG
Mojastin [P0C7X7]           EAGEECDCGSPANPCCDAATCKLRPGAQCADGLCCDQCRFIKKGTVCRPARGDWNDDTCTGQSADCPRNGLYG
Horrdistatin [P0C7X6]       --GEECDCGSPANPCCDAATCKLRPGAQCADGLCCDQCRFIKKGTVCRPARGDWNDDTCTGQSADCPRNGLYG
```

Fig. 5. Amino acid sequence comparison of *C. s. tzabcan* disintegrins with selected disintegrins; RGDN disintegrins are in the top group and RGDW disintegrins are in the bottom diagram. One-letter code for amino acids is used. Cysteine residues are shaded in gray, and the RGD binding motif is in bold print and underlined. Residue differences from tzabcanin are shaded in yellow.

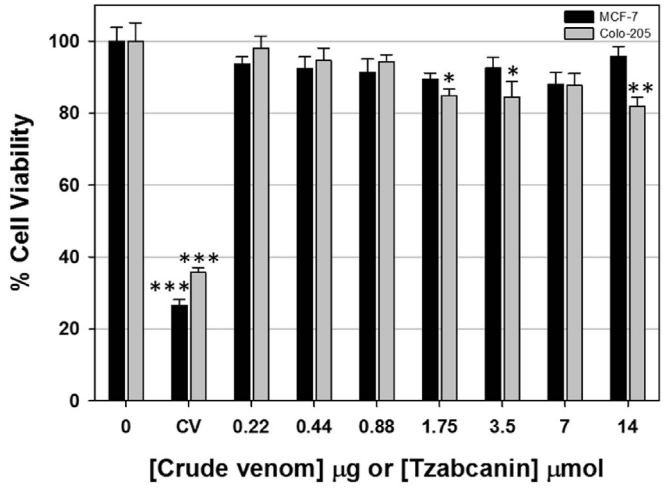

Fig. 6. Percent cell viability of Colo-205 and MCF-7 cells following exposure to crude *C. s. tzabcan* venom (CV) or purified tzabcanin. *p < 0.05, **p < 0.01, ***p < 0.001, compared to controls.

high affinity to $\alpha_{IIb}\beta_3$ integrins, whereas RGDN show higher selectivity towards both $\alpha_5\beta_1$ and $\alpha_v\beta_3$ integrins [16,17,47]. Of the six disintegrins reported here, four contain an RGDW binding motif, and two, including tzabcanin, contain an RGDN binding region. Yet even with identical integrin-binding regions, structural discrepancies in the C-terminal region can alter biological activity. Differences in ADP-induced platelet aggregation have been documented between colombistatin and cotiarin, both RGDN disintegrins that differ only by the presence of a Tyr72 in colombistatin, whereas cotiarin exhibits His72 [23].

Although crude *C. s. tzabcan* venom was highly toxic to both Colo-205 or MCF-7 cell lines, purified tzabcanin showed very low levels of cytotoxicity toward Colo-205 cells and failed to exhibit cytotoxicity at concentrations as high as 14 μM following 24 h treatment of MCF-7 cells. Disintegrin-induced apoptosis in HUVEC cells has been documented with rhodostomin [48] as well as with accutin [49]; however, the ability of disintegrins to induce apoptosis varies between cancer cell lines. Lucena et al. [29] found that the recombinant RGDN disintegrin, r-viridistatin, failed to induce apoptosis in SK-12 melanoma cells, and the disintegrin rhodostomin did not induce apoptosis of MDA-MB-231 cells [50].

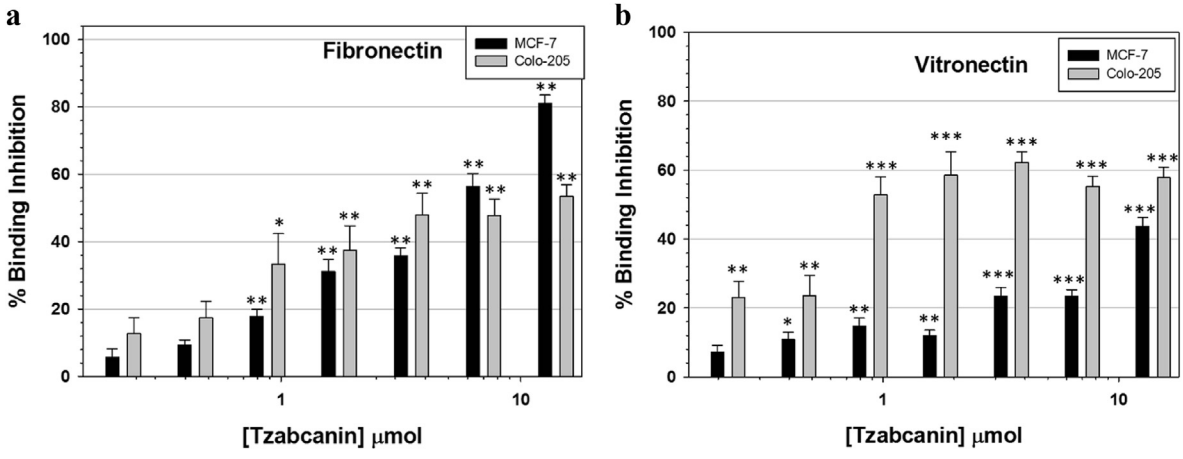

Fig. 7. a The effect of tzabcanin on Colo-205 and MCF-7 adhesion to immobilized fibronectin; semilog plot. Various concentrations of tzabcanin (0.22 μM–14 μM) were incubated with Colo-205 and MCF-7 cells (5.0×10^5 cells/mL) prior to addition to 96-well culture plates containing immobilized fibronectin. *p < 0.01, **p < 0.001. b. The effects of tzabcanin on Colo-205 and MCF-7 adhesion to immobilized vitronectin; semilog plot. Various concentrations of tzabcanin (0.22 μM–14 μM) were incubated with Colo-205 and MCF-7 cells (5.0×10^5 cells/mL) prior to addition to 96-well culture plates containing immobilized vitronectin. *p < 0.05, **p < 0.01, ***p < 0.001, relative to controls.

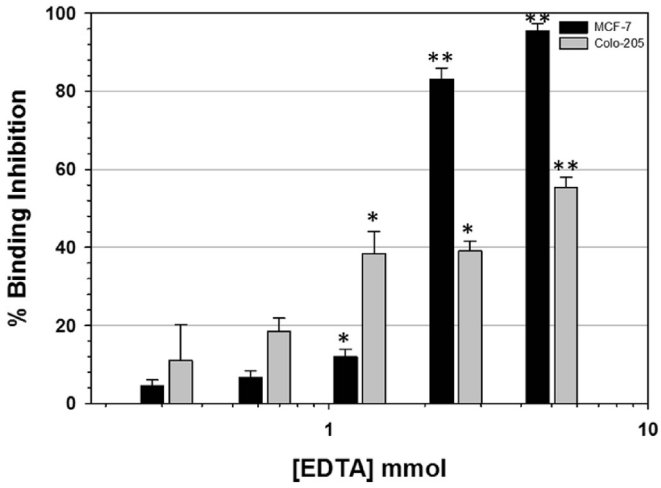

Fig. 8. Percent binding inhibition of Colo-205 and MCF-7 cells to immobilized tzabcanin following cell incubation with the cation chelator EDTA; semilog plot. Colo-205 and MCF-7 cells (5.0×10^5 cells/mL) were incubated with various concentrations of EDTA (0.3–5 mM) prior to addition to wells containing immobilized tzabcanin. $^{*}p < 0.01$, $^{**}p < 0.001$, relative to controls.

Similarly, the homodimeric disintegrin contortrostatin was found to lack cytotoxicity toward MDA-MB-435 cells *in vitro* [22]. However, recently Lucena et al. [30] showed that recombinant disintegrins r-virdistatin 2 and r-mojastin 1 induced apoptosis in approximately 20% of human pancreatic adenocarcinoma (BXPC-3) cells. Therefore, the slight decrease in Colo-205 cell viability in the presence of high concentrations of tzabcanin could be due to induction of apoptosis, or a loss of membrane integrity, ultimately leading to antiproliferative effects. On the other hand, the potent toxicity of crude venom towards both cell lines is likely due to the presence of LAAOs, SVMPs, and PLA_2s, which are abundant in *C. s. tzabcan* venom [51] and have been shown to exhibit a combination of cytotoxic and apoptotic activities [52–54]. Similarly, Bradshaw et al. [38] also showed that *C. s. tzabcan* venom was significantly cytotoxic to both MCF-7 and human melanoma (A-375) cell lines.

Integrins are critical to cell attachment, migration and invasion, and their significance in cancer progression is being examined extensively [55,56]. Integrin engagement to ECM proteins induces cell proliferation and may prevent apoptosis in some cancers, demonstrating the significance of cell adhesion in tumor progression and survival. α_v integrins, in addition to $\alpha_5\beta_1$, $\alpha_8\beta_1$, and $\alpha_{IIb}\beta_3$, mediate cell adhesion to various ECM proteins, often by recognition of the tri-peptide RGD binding motif [57]. These integrin-ligand interactions are dependent on divalent cations, especially Mn^{2+} and Mg^{2+}, to support ligand binding [40]. Ca^{2+}, on the other hand, fails to support binding, yet it greatly regulates ligand adhesion supported by Mn^{2+} and Mg^{2+} [40]. The inhibition of both Colo-205 and MCF-7 cell binding to immobilized tzabcanin in the presence of a cation chelator (EDTA) indicates that tzabcanin-integrin binding was occurring, likely through the RGD domain. The low binding inhibition seen in Colo-205 cells (~55% binding inhibition at 5 mM EDTA) compared to MCF-7 cells suggests that tzabcanin binding is occurring in this cell line through a higher number of integrins, requiring a higher concentration of EDTA to produce inhibition. Although tzabcanin binds to both Colo-205 and MCF-7 cells, tzabcanin-induced binding inhibition of these cell lines to fibronectin and vitronectin is not as potent as has been reported for some other disintegrins. Differential potency may be cell line dependent; for example, colombistatin had a potent inhibitory effect ($IC_{50} = 33$ nM) on SK-Mel-28 cell adhesion to fibronectin, yet much higher concentrations ($IC_{50} = 4.4$ μM) of this disintegrin were needed to inhibit T24 cells from binding to fibronectin [23]. A recombinant form of viridistatin-2 also showed varying binding inhibition of numerous cell lines to fibronectin, with IC_{50} values ranging from 11 to 4450 nM [29]. Further, although inhibition of cell adhesion was not as potent as other disintegrins, tzabcanin may exhibit additional anti-metastatic properties by binding different integrin receptors. For example, crotatroxin 2 failed to inhibit 66.3p cell adhesion to fibronectin, yet it significantly inhibited cell migration *in vitro* and lung tumor colonization *in vivo* [27].

Colo-205 and MCF-7 cells express integrins $\alpha_5\beta_1$, $\alpha_v\beta_5$ and $\alpha_v\beta_6$, as well as several other α/β subunits [58–61]; however, the expression of these integrins and specific subunits may drastically vary. For instance, Colo-205 cells show low levels of α_5, but moderate levels of α_v, α_1, and α_3, and high levels of α_2, α_6 and β_1 subunits [58], each displaying specificity to one or several discrete ligands. Fibronectin is recognized by an array of integrins including $\alpha_5\beta_1$ and $\alpha_v\beta_6$, which were first characterized for their ability to bind to this ECM protein [62–64]. Integrins $\alpha_v\beta_3$, $\alpha_v\beta_5$, $\alpha_3\beta_1$ $\alpha_4\beta_1$ and $\alpha_8\beta_1$ are additional receptors of fibronectin [65]. Fibronectin-integrin interactions contribute to numerous stages of tumor development, including tumor migration, invasion and metastasis [66]. $\alpha_v\beta_5$ has classically been known as a vitronectin receptor [67,68] however, integrin $\alpha_v\beta_6$ has also been shown to adhere to vitronectin [69]. Therefore, Colo-205 and MCF-7 cells express an array of integrins that show recognition to both fibronectin and vitronectin.

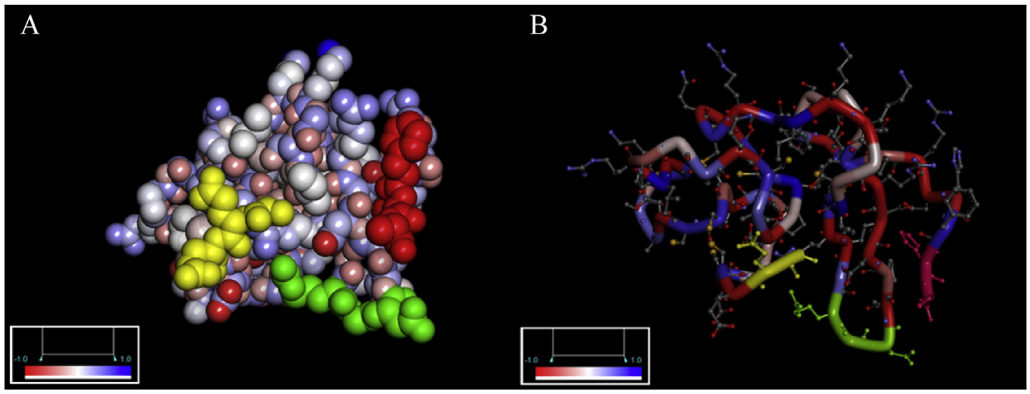

Fig. 9. Space filling model (A) and stick model (B) of tzabcanin showing the same face of the molecule. In both figures, the RGD domain is shown in green, the N terminus is in yellow and the C terminus is shown in red. Surface charges of other residues are shown in red to blue shading. Models are based on I-TASSER-derived modeling of tzabcanin and were constructed using Accelerys Discovery Studio 3.1 software. Note proximity of the RDG domain and the C-terminus.

Because many disintegrins have the capability to recognize an array of integrins, the relatively weak potency of tzabcanin suggest that this disintegrin may inhibit cell adhesion by binding to a more select group of integrins, leaving other receptors available for integrin-ECM interactions. Further, tzabcanin also contains an RGDN binding domain which has been shown to exhibit higher affinity to integrin $\alpha_v\beta_3$ [16,47], an integrin not expressed on either Colo-205 or MCF-7 cells. Therefore, studies utilizing cell lines expressing $\alpha_v\beta_3$ are predicted to demonstrate greater potency of tzabcanin.

5. Conclusions

This study reports the isolation and characterization of the most abundant disintegrin, tzabcanin, from the venom of *C. s. tzabcan*. In addition, we report molecular masses and cDNA sequences of five additional medium-sized disintegrin isoforms from the same venom. The documented differences in integrin-binding affinity between RGDW and RGDN disintegrins could represent distinct biological roles for these integrin homologs and differential anti-cancer effects may also exist. Tzabcanin, a new RGD disintegrin, was not cytotoxic to MCF-7 cells but produced a slight decrease in cell viability in Colo-205 cells at high concentrations. This could be due to induction of apoptosis by binding to an integrin(s) specifically expressed on Colo-205 cells that may be absent on the MCF-7 cell line. By binding to integrins, tzabcanin also inhibited cell adhesion of both cell lines to fibronectin and vitronectin. Although this inhibition was not as potent as reported for other disintegrins, the binding domain (RGDN) of tzabcanin suggests that it may have higher affinity towards $\alpha_v\beta_3$ integrins which are not present in either Colo-205 or MCF-7 cells.

Conflict of interest statement

The authors declare that there are no conflicts of interest.

Acknowledgments

This work was supported by grants from the Colorado Office of Economic Development and International Trade (11BGF-10) and from the UNC Provost fund. We thank Patrick Burns and Ashis Mukherjee for their assistance with several aspects of this project.

References

[1] S.P. Mackessy, The field of reptile toxinology: snakes, lizards, and their venoms, in: S.P. Mackessy (Ed.), Handbook of Venoms and Toxins of Reptiles, CRC Press/Taylor & Francis Group, Boca Rotan, 2010, pp. 3–23.
[2] K.V. Kardong, T.L. Kiene, V. Bels, Evolution of trophic systems in squamates, Neth. J. Zool. 47 (1996) 411–427.
[3] J.W. Fox, S.M. Serrano, Approaching the golden age of natural product pharmaceuticals from venom libraries: an overview of toxins and toxin-derivatives currently involved in therapeutic or diagnostic applications, Curr. Pharm. Des. 13 (2007) 2927–2934, http://dx.doi.org/10.2174/138161207782023739.
[4] F.J. Vonk, K. Jackson, R. Doley, F. Madaras, P.J. Mirtschin, N. Vidal, Snake venom: from fieldwork to the clinic, Bioessays 33 (2011) 269–279, http://dx.doi.org/10.1002/bies.201000117.
[5] A.J. Saviola, M.E. Peichoto, S.P. Mackessy, Rear-fanged snake venoms: an untapped source of novel compounds and potential drug leads, Toxin Rev. 33 (2014) 185–201, http://dx.doi.org/10.3109/15569543.2014.942040.
[6] R.M. Kini, H.J. Evans, Structural domains in venom proteins: evidence that metalloproteinases and nonenzymatic platelet aggregation inhibitors (disintegrins) from snake venoms are derived by proteolysis from a common precursor, Toxicon 30 (1992) 265–293.
[7] C. Ouyang, H.-I. Yeh, T.-F. Huang, A potent platelet aggregation inhibitor purified from *Agkistrodon halys* (Mamushi) snake venom, Toxicon 21 (1983) 797–804.
[8] R.J. Gould, M.A. Polokoff, P.A. Friedman, T.-F. Huang, J.C. Holt, J.J. Cook, et al., Minireview. Disintegrins: a family of integrin inhibitory proteins from viper venoms, Proc. Soc. Exp. Biol. Med. 195 (1990) 168–171, http://dx.doi.org/10.3181/00379727-195-43129B.
[9] A.J. Saviola, D. Chiszar, C. Busch, S.P. Mackessy, Molecular basis for prey relocation in viperid snakes, BMC Biol. 11 (2013) 20, http://dx.doi.org/10.1186/1741-7007-11-20.
[10] J. Calvete, M. Moreno-Murciano, R. Theakston, D. Kisiel, C. Marcinkiewicz, Snake venom disintegrins: novel dimeric disintegrins and structural diversification by disulphide bond engineering, Biochem. J. 372 (2003) 725–734, http://dx.doi.org/10.1042/BJ20021739.
[11] J.J. Calvete, C. Marcinkiewicz, D. Monleón, V. Esteve, B. Celda, P. Juárez, et al., Snake venom disintegrins: evolution of structure and function, Toxicon 45 (2005) 1063–1074, http://dx.doi.org/10.1016/j.toxicon.2005.02.024.
[12] R.M. Cooke, B.G. Carter, P. Murray-Rust, M.J. Hartshorn, P. Herzyk, R.E. Hubbard, The solution structure of echistatin: evidence for disulphide bond rearrangement in homologous snake toxins, Protein Eng. 5 (1992) 473–477, http://dx.doi.org/10.1093/protein/5.6.473.
[13] D. Monleón, V. Esteve, H. Kovacs, J. Calvete, B. Celda, Conformation and concerted dynamics of the integrin-binding site and the C-terminal region of echistatin revealed by homonuclear NMR, Biochem. J. 387 (2005) 57–66, http://dx.doi.org/10.1042/BJ20041343.
[14] J.J. Calvete, C. Marcinkiewicz, L. Sanz, KTS and RTS-disintegrins: anti-angiogenic viper venom peptides specifically targeting the α1β 1 integrin, Curr. Pharm. Des. 13 (2007) 2853–2859, http://dx.doi.org/10.2174/138161207782023766.
[15] E.M. Walsh, C. Marcinkiewicz, Non-RGD-containing snake venom disintegrins, functional and structural relations, Toxicon 58 (2011) 355–362, http://dx.doi.org/10.1016/j.toxicon.2011.07.004.
[16] R.M. Scarborough, J.W. Rose, M.A. Naughton, D.R. Phillips, L. Nannizzi, A. Arfsten, et al., Characterization of the integrin specificities of disintegrins isolated from American pit viper venoms, J. Biol. Chem. 268 (1992) 1058–1065.
[17] P. Juárez, I. Comas, F. González-Candelas, J.J. Calvete, Evolution of snake venom disintegrins by positive Darwinian selection, Mol. Biol. Evol. 25 (2008) 2391–2407, http://dx.doi.org/10.1093/molbev/msn179.
[18] J.J. Calvete, Structure-function correlations of snake venom disintegrins, Curr. Pharm. Des. 11 (2005) 829–835, http://dx.doi.org/10.2174/1381612053381783.
[19] M. Brown, J. Eble, J. Calvete, C. Marcinkiewicz, Structural requirements of KTS-disintegrins for inhibition of alpha1beta1 integrin, Biochem. J. 417 (2009) 95–101, http://dx.doi.org/10.1042/BJ20081403.
[20] D.G. Kisiel, J.J. Calvete, J. Katzhendler, A. Fertala, P. Lazarovici, C. Marcinkiewicz, Structural determinants of the selectivity of KTS-disintegrins for the a11 integrin, FEBS Lett. 577 (2004) 478–482, http://dx.doi.org/10.1016/j.febslet.2004.10.050.
[21] M. Trikha, Y.A. De Clerck, F.S. Markland, Contortrostatin, a snake venom disintegrin, inhibits β1 integrin-mediated human metastatic melanoma cell adhesion and blocks experimental metastasis, Cancer Res. 54 (1994) 4993–4998.
[22] Q. Zhou, R.P. Sherwin, C. Parrish, V. Richters, S.G. Groshen, D. Tsao-Wei, et al., Contortrostatin, a dimeric disintegrin from *Agkistrodon contortrix contortrix*, inhibits breast cancer progression, Breast Cancer Res. Treat. 61 (2000) 249–259, http://dx.doi.org/10.1023/A:1006457903545.
[23] E.E. Sánchez, A. Rodríguez-Acosta, R. Palomar, S.E. Lucena, S. Bashir, J.G. Soto, et al., Colombistatin: a disintegrin isolated from the venom of the South American snake (*Bothrops colombiensis*) that effectively inhibits platelet aggregation and SK-Mel-28 cell adhesion, Arch. Toxicol. 83 (2009) 271–279, http://dx.doi.org/10.1007/s00204-008-0358-y.
[24] Y. Angulo, A. Castro, B. Lomonte, A. Rucavado, J. Fernández, J.J. Calvete, et al., Isolation and characterization of four medium-size disintegrins from the venoms of Central American viperid snakes of the genera *Atropoides*, *Bothrops*, *Cerrophidion*, and *Crotalus*, Biochimie 107 (2014) 376–384, http://dx.doi.org/10.1016/j.biochi.2014.10.010.
[25] Z.R. Gan, R.J. Gould, J.W. Jacobs, P.A. Friedman, M.A. Polokoff, Echistatin. A potent platelet aggregation inhibitor from the venom of the viper, *Echis carinatus*, J. Biol. Chem. 263 (1988) 19827–19832.
[26] Q. Zhou, M.T. Nakada, C. Arnold, K.Y. Shieh, F.S. Markland Jr., Contortrostatin, a dimeric disintegrin from *Agkistrodon contortrix contortrix*, inhibits angiogenesis, Angiogenesis 3 (1999) 259–269, http://dx.doi.org/10.1023/A:1009059210733.
[27] J.A. Galan, E.E. Sánchez, A. Rodríguez-Acosta, J.G. Soto, S. Bashir, M.A. McLane, et al., Inhibition of lung tumor colonization and cell migration with the disintegrin crotatroxin 2 isolated from the venom of Crotalus atrox, Toxicon 51 (2008) 1186–1196, http://dx.doi.org/10.1016/j.toxicon.2008.02.004.
[28] S. Lucena, E.E. Sánchez, J.C. Perez, Anti-metastatic activity of the recombinant disintegrin, r-mojastin 1, from the Mohave rattlesnake, Toxicon 57 (2011) 794–802, http://dx.doi.org/10.1016/j.toxicon.2011.02.014.
[29] S.E. Lucena, Y. Jia, J.G. Soto, J. Parral, E. Cantu, J. Brannon, et al., 2012. Anti-invasive and anti-adhesive activities of a recombinant disintegrin, r-viridistatin 2, derived from the Prairie rattlesnake (*Crotalus viridis viridis*), Toxicon 60 (2012) 31–39, http://dx.doi.org/10.1016/j.toxicon.2012.03.011.
[30] S. Lucena, R. Castro, C. Lundin, A. Hofstetter, A. Alaniz, M. Suntravat, et al., Inhibition of pancreatic tumoral cells by snake venom disintegrins, Toxicon 93 (2015) 136–143, http://dx.doi.org/10.1016/j.toxicon.2014.11.228.
[31] C. Marcinkiewicz, P.H. Weinreb, J.J. Calvete, D.G. Kisiel, S.A. Mousa, G.P. Tuszynski, R.R. Lobb, Obtustatin A potent selective inhibitor of α1β1 integrin in vitro and angiogenesis in vivo, Cancer Res. 63 (2003) 2020–2023.

[32] M.C. Brown, I. Staniszewska, L. Del Valle, G.P. Tuszynski, C. Marcinkiewicz, Angiostatic activity of obtustatin as a1b1 integrin inhibitor in experimental melanoma growth, Int. J. Cancer 123 (2008) 2195–2203, http://dx.doi.org/10.1002/ijc.23777.
[33] S.P. Mackessy, Venom ontogeny in the Pacific rattlesnakes *Crotalus viridis helleri* and C. v. oreganus, Copeia (1988) 92–101.
[34] C.L. Weldon, S.P. Mackessy, Biological and proteomic analysis of venom from the Puerto Rican Racer (*Alsophis portoricensis*: Dipsadidae), Toxicon 55 (2010) 558–569, http://dx.doi.org/10.1016/j.toxicon.2009.10.010.
[35] M. Suntravat, Y. Jia, S.E. Lucena, E.E. Sánchez, J.C. Pérez, cDNA cloning of a snake venom metalloproteinase from the eastern diamondback rattlesnake (*Crotalus adamanteus*), and the expression of its disintegrin domain with anti-platelet effects, Toxicon 64 (2013) 43–54, http://dx.doi.org/10.1016/j.toxicon.2012.12.025.
[36] J. Durban, P. Juárez, Y. Angulo, B. Lomonte, M. Flores-Diaz, A. Alape-Girón, et al., Profiling the venom gland transcriptomes of Costa Rican snakes by 454 pyrosequencing, BMC Genomics 12 (2011) 259, http://dx.doi.org/10.1186/1471-2164-12-259.
[37] T. Mosmann, Rapid colorimetric assay for cellular growth and survival: application to proliferation and cytotoxicity assays, J. Immunol. Methods 65 (1983) 55–63.
[38] M.J. Bradshaw, A.J. Saviola, E. Fesler, S.P. Mackessy, Evaluation of cytotoxic activities of snake venoms toward breast (MCF-7) and skin cancer (A-375) cell lines, Cytotechnology (2014) 1–14, http://dx.doi.org/10.1007/s10616-014-9820-2 (early release).
[39] I. Wierzbicka-Patynowski, S. Niewiarowski, C. Marcinkiewicz, J.J. Calvete, M.M. Marcinkiewicz, M.A. McLane, Structural requirements of echistatin for the recognition of $\alpha_v\beta_3$ and $\alpha_5\beta_1$ integrins, J. Biol. Chem. 274 (1999) 37809–37814, http://dx.doi.org/10.1074/jbc.274.53.37809.
[40] A.P. Mould, S.K. Akiyama, M.J. Humphries, Regulation of integrin α5β1-fibronectin interactions by divalent cations: evidence for distinct classes of binding sites for Mn^{2+}, Mg^{2+}, and Ca^{2+}, J. Biol. Chem. 270 (1995) 26270–26277, http://dx.doi.org/10.1074/jbc.270.44.26270.
[41] S. Tiwari, J.A. Askari, M.J. Humphries, N.J. Bulleid, Divalent cations regulate the folding and activation status of integrins during their intracellular trafficking, J. Cell Sci. 124 (2011) 1672–1680, http://dx.doi.org/10.1242/jcs.084483.
[42] W.H. Heyborne, S.P. Mackessy, Identification and characterization of a taxon-specific three-finger toxin from the venom of the Green Vinesnake (*Oxybelis fulgidus*; family Colubridae), Biochimie 95 (2013) 1923–1932, http://dx.doi.org/10.1016/j.biochi.2013.06.025.
[43] J. Shin, W. Lee, Solution structure of a novel disintegrin, salmosin, from *Agkistrondon halys* venom, Biochemistry 42 (2003) 14408–14415.
[44] J.W. Fox, S.M. Serrano, Snake venom metalloproteinases, in: S.P. Mackessy (Ed.), Handbook of Venoms and Toxins of Reptiles, CRC Press/Taylor & Francis Group, Boca Rotan, 2010, pp. 95–114.
[45] J.M. Gutiérrez, A. Rucavado, T. Escalante, Snake venom metalloproteinases: biological roles and participation in the pathophysiology of envenomation, in: S.P. Mackessy (Ed.), Handbook of Venoms and Toxins of Reptiles, CRC Press/Taylor & Francis Group, Boca Rotan, 2010, pp. 115–138.
[46] D. Okuda, H. Koike, T. Morita, A new gene structure of the disintegrin family: a subunit of dimeric disintegrin has a short coding region, Biochemistry 41 (2002) 14248–14254, http://dx.doi.org/10.1021/bi025876s.
[47] C. Marcinkiewicz, S. Vijay-Kumar, M.A. McLane, S. Niewiarowski, Significance of RGD loop and C-terminal domain of echistatin for recognition of αIIbβ3 and αvβ3 integrins and expression of ligand-induced binding site, Blood 90 (1997) 1565–1575.
[48] C.H. Yeh, H.C. Peng, R.S. Yang, T.F. Huang, Rhodostomin, a snake venom disintegrin, inhibits angiogenesis elicited by basic fibroblast growth factor and suppresses tumor growth by a selective αvβ3 blockade of endothelial cells, Mol. Pharm. 59 (2001) 1333–1342, http://dx.doi.org/10.1124/mol.59.5.1333.
[49] C.H. Yeh, H.C. Peng, T.F. Huang, Accutin, a new disintegrin, inhibits angiogenesis *in vitro* and *in vivo* by acting as integrin αvβ3 antagonist and inducing apoptosis, Blood 92 (1998) 3268–3276.
[50] R.S. Yang, C.H. Tang, W.J. Chuang, T.H. Huang, H.C. Peng, T.F. Huang, et al., Inhibition of tumor formation by snake venom disintegrin, Toxicon 45 (2005) 661–669, http://dx.doi.org/10.1016/j.toxicon.2005.01.013.
[51] E.N. Castro, B. Lomonte, M.C. Gutierrez, A. Alagon, J.M. Gutierrez, Intraspecies variation in the venom of the rattlesnake *Crotalus simus* from Mexico: different expression of crotoxin results in highly variable toxicity in the venoms of three subspecies, J. Proteomics 87 (2013) 103–121, http://dx.doi.org/10.1016/j.jprot.2013.05.024.
[52] L.H. Gremski, O.M. Chaim, K.S. Paludo, Y.B. Sade, M.F. Otuki, M. Richardson, et al., Cytotoxic, thrombolytic and edematogenic activities of leucurolysin-a, a metalloproteinase from *Bothrops leucurus* snake venom, Toxicon 50 (2007) 120–134, http://dx.doi.org/10.1016/j.toxicon.2007.03.002.
[53] M.L. Lee, S.Y. Fung, I. Chung, J. Pailoor, S.H. Cheah, N.H. Tan, King Cobra (*Ophiophagus hannah*) venom L-amino acid oxidase induces apoptosis in PC-3 cells and suppresses PC-3 solid tumor growth in a tumor xenograft mouse model, Int. J. Med. Sci. 11 (2014) 593–601, http://dx.doi.org/10.7150/ijms.8096.
[54] D. Mora-Obando, J. Fernandez, C. Montecucco, J.M. Gutiérrez, B. Lomonte, Synergism between basic Asp49 and Lys49 phospholipase A_2 myotoxins of viperid snake venom *in vitro* and in vivo, PloS One 9 (2014) e109846, http://dx.doi.org/10.1371/journal.pone.0109846.
[55] G.J. Mizejewski, Role of integrins in cancer: survey of expression patterns, Exp. Biol. Med. 222 (1999) 124–138.
[56] J.S. Desgrosellier, D.A. Cheresh, Integrins in cancer: biological implication and therapeutic opportunities, Nat. Rev. Cancer 10 (2010) 9–22, http://dx.doi.org/10.1038/nrc2748.
[57] E.H.J. Danen, A. Sonnenberg, Integrins in regulation of tissue development and function, J. Pathol. 200 (2003) 471–480, http://dx.doi.org/10.1002/path.1472.
[58] K. Koretz, S. Brüderlein, C. Henne, T. Fietz, M. Laque, P. Möller, Comparative evaluation of integrin α-and β-chain expression in colorectal carcinoma cell lines and in their tumours of origin, Virchows Arch. 425 (1994) 229–236, http://dx.doi.org/10.1007/BF00196144.
[59] M.V. Agrez, R.C. Bates, D. Mitchell, N. Wilson, N. Ferguson, P. Anseline, et al., Multiplicity of fibronectin-binding alpha V integrin receptors in colorectal cancer, Br. J. Cancer 73 (1996) 887–892.
[60] R. Korah, M. Boots, R. Wieder, Integrin α5β1 promotes survival of growth-arrested breast cancer cells an in vitro paradigm for breast cancer dormancy in bone marrow, Cancer Res. 64 (2004) 4514–4522, http://dx.doi.org/10.1158/0008-5472.CAN-03-3853.
[61] A. Taherian, X. Li, Y. Liu, T.A. Haas, Differences in integrin expression and signaling within human breast cancer cells, BMC Cancer 11 (2001) 293, http://dx.doi.org/10.1186/1471-2407-11-293.
[62] Y. Takada, C. Huang, M.E. Hemler, Fibronectin receptor structures in the VLA family of heterodimers, Nature 326 (1987) 607–609, http://dx.doi.org/10.1038/326607a0.
[63] E. Rouslahti, Fibronectin and its receptors, Annu. Rev. Biochem. 57 (1988) 375–413, http://dx.doi.org/10.1146/annurev.bi.57.070188.002111.
[64] M. Busk, R. Pytela, D. Sheppard, Characterization of the integrin alpha v beta 6 as a fibronectin-binding protein, J. Biol. Chem. 267 (1992) 5790–5796.
[65] A.M. Mourshi, R.K. Globus, C.H. Damsky, Interactions between integrin receptors and fibronectin are required for calvarial osteoblast differentiation *in vitro*, J. Cell Sci. 110 (1997) 2187–2196.
[66] S.K. Akiyama, K. Olden, K.M. Yamada, Fibronectin and integrins in invasion and metastasis, Cancer Metastasis Rev. 14 (1995) 173–189, http://dx.doi.org/10.1007/BF00690290.
[67] D.A. Cheresh, J.W. Smith, H.M. Cooper, V. Quaranta, A novel vitronectin receptor integrin ($\alpha_v\beta_x$) is responsible for distinct adhesive properties of carcinoma cells, Cell 57 (1989) 59–69.
[68] J.W. Smith, D.J. Vestal, S.V. Irwin, T.A. Burke, D.A. Cheresh, Purification and functional characterization of integrin alpha v beta 5. An adhesion receptor for vitronectin, J. Biol. Chem. 265 (1990) 11008–11013.
[69] X. Huang, J. Wu, S. Spong, D. Sheppard, The integrin αvβ6 is critical for keratinocyte migration on both its known ligand, fibronectin, and on vitronectin, J. Cell Sci. 111 (1998) 2189–2195.